The influence of thermal vibrations on the average structure of cubic $NaMgF_3$ perovskite: a combined molecular dynamics and neutron diffraction study

1997 J. Phys.: Condens. Matter 9 L647

(http://iopscience.iop.org/0953-8984/9/50/001)

J. Phys.: Condens. Matter **9** (1997) L647–L655. Printed in the UK PII: S0953-8984(97)88322-1

LETTER TO THE EDITOR

The influence of thermal vibrations on the average structure of cubic $NaMgF_3$ perovskite: a combined molecular dynamics and neutron diffraction study

J N Street†, I G Wood†, K S Knight‡ and G D Price†

† Research School of Geological and Geophysical Sciences, Birkbeck College and University College London, Gower Street, London WC1E 6BT, UK

‡ ISIS Facility, Rutherford Appleton Laboratory, Chilton, Didcot OX11 0QX, UK

Received 10 October 1997

Abstract. The structure of $NaMgF_3$ has been investigated by high-temperature neutron diffraction and molecular dynamics simulation. It was found that the apparent Mg–F bond contraction reported in previous work arises from large anisotropy in the distribution of F^- ions. The cell parameter in the cubic phase is approximately 2% less than twice the average Mg–F bond distance. The consequences for computer simulation of perovskites of this dynamically induced reduction in cell volume are briefly discussed.

The petrology of the Earth's lower mantle is thought to be determined by $(Mg, Fe)SiO_3$ perovskite [1] and the physical properties of this mineral are, therefore, of great interest within the Earth sciences [2]. However, due to the very high pressures and temperatures necessary to perform experiments at lower-mantle conditions, the behaviour of $(Mg, Fe)SiO_3$ is not easily investigated. One approach to overcoming these difficulties is to use a combination of computer simulation [3–5] with experimental studies of structurally similar compounds [6]. Neighborite, $NaMgF_3$ perovskite [7], provides potentially one of the best analogue materials as it is isoelectronic with $MgSiO_3$ and shows the same orthorhombic ($Pbnm$) distortion from the ideal cubic aristotype at room temperature.

There have been a number of recent investigations of $NaMgF_3$, including a molecular dynamics simulation [8] and structural studies by x-ray powder diffraction at high temperatures [9, 10], high pressures [11] and simultaneous high pressures and temperatures [12]. There are, however, at least three aspects of the behaviour of this material for which our understanding is far from complete. Firstly, there is the question of whether $NaMgF_3$ becomes a superionic conductor at temperatures close to its melting point ($T_m \approx 1303$ K) as a result of anion sublattice melting. The available experimental data are contradictory, with earlier work [13] suggesting ionic conduction for $T > 0.9T_m$ but later work [14] reporting no evidence for superionicity at temperatures up to $0.98T_m$. Similarly, an early molecular dynamics investigation [15] found neither cation nor anion diffusion, even under conditions of strong superheating, whereas more recent work [8] indicated anionic superionicity for temperatures above about $0.92T_m$, similar to that reported for $MgSiO_3$ [16].

The second feature of interest in $NaMgF_3$ is the number and nature of its structural phase transitions. X-ray powder diffraction studies [9, 10] have shown that the material transforms directly from the room-temperature orthorhombic ($Pbnm$) structure to the cubic ($Pm3m$) aristotype at about 1040 K (T_c) and that the transition appears to be continuous. Application

0953-8984/97/500647+09$19.50

of pressure [11, 12] indicated that this direct $Pbnm \rightarrow Pm3m$ transition occurred at all pressures (with T_c increasing by 45 K GPa^{-1}) and that, whereas the dominant mechanism for thermal expansion was a decrease in the octahedral tilting, the dominant compression mechanism was a reduction in size of the MgF_6 octahedra. The usual origin of transitions resulting from octahedral tilting in perovskites is soft-mode condensation [17, 18], especially the so-called M_3 mode at the M point of the Brillouin zone of the cubic aristotype, with wavevector $(110)\pi/a$, and the R_{25} mode at the R point, $(111)\pi/a$. Both of these modes involve rotations of the octahedra about the ⟨100⟩ directions of the cubic phase, with adjacent octahedra tilted in opposite senses in the plane perpendicular to the rotation axis. In the singlet M_3 mode the tilts along the rotation axis are in the same sense, whereas in the triply degenerate R_{25} mode they are in the opposite sense. Using Glazer's notation [19] condensation of an M-point mode will produce a tilt system of the form $a^0a^0c^+$, whereas condensation of a component of an R-point mode will result in $a^0a^0c^-$. The tilt system in orthorhombic $NaMgF_3$ is of the form $a^-a^-c^+$ and thus simultaneous condensation of two normal modes with different wavevector is required for this structure to result from a direct transition from the cubic phase. This suggests [18] that the whole phonon branch from the R to the M point involving octahedral rotations may soften, with strong mode coupling; it also implies that the transition must be formally of first order [20]. X-ray diffraction [10] indicates that if an intermediate tetragonal or orthorhombic phase exists between the $Pm3m$ and $Pbnm$ structures it must be present for only a very small temperature interval, of perhaps 1–2 K. Further accurate lattice parameter measurements and, ideally, inelastic neutron scattering experiments would be required to investigate these details.

The final unusual feature of the behaviour of $NaMgF_3$, towards which this present paper is addressed, is the anomalous Mg–F bond contraction close to T_c reported by Zhao *et al* [9, 12], in which the apparent Mg–F bond length (as determined from x-ray powder diffraction) shortened by about 0.02 Å, with increasing temperature, over a range of roughly 100 K below T_c. An actual contraction of the bond did not seem physically reasonable and Zhao *et al* [9] postulated that the effect was due to thermal vibration, suggesting in their extended discussion of perovskite structures in general that 'the volume of the cubic form of $MgSiO_3$ is probably overestimated by assuming that the cell edge is twice the expected (Si–O) bond length'. They were, however, unable to fully quantify their discussion. In the present work, we use a combination of molecular dynamics, together with a determination of the average cubic structure of $NaMgF_3$ by powder neutron diffraction to show that the probability density of fluorine ions is very anisotropic and that this leads to a cell parameter which is approximately 2% less than twice the average Mg–F bond distance.

The powder sample for neutron diffraction was prepared by sintering a stoichiometric mixture of NaF and MgF_2 (nominally 99.99% purity) at 750 °C for 15 h. The neutron diffraction experiment was carried out using the high-resolution time-of-flight diffractometer (HRPD) at the ISIS facility, Rutherford Appleton Laboratories (RAL). The sample was held in a vanadium can, under vacuum, and the heating elements in the furnace were also constructed from vanadium. The diffraction pattern was measured at 1223 K ($\approx 0.94T_m$); the temperature stability was ±0.1 K. Data were collected in back-scattering geometry, for d-spacings in the range $0.3 < d < 2.1$ Å, over a period of approximately 6.5 h. Data reduction and structure refinements were carried out using the RAL's suite of programs based on the Cambridge Crystallography Subroutine Library (CCSL) [21–23]. In analysing the diffraction pattern an initial CAILS (cell and intensity least-squares) refinement was used to determine the cell, background and halfwidth parameters (this method of analysis assumes nothing about the crystal structure other than its space group and should, therefore, give an unbiased set of cell parameters and halfwidths etc). This was then followed by

a Rietveld refinement in which only the scale factor, anisotropic temperature factors for all atoms and an extinction length were allowed to vary, giving six parameters in all. The results of the refinement are shown in table 1. The model fitted the data very well ($\chi^2 = 1.2$) and all positional parameters are fixed by symmetry. We consider, therefore, that the thermal parameters are accurately determined. Fourier maps (figure 3) were calculated using the observed structure factor values derived from the Rietveld refinement, using those reflections for which $d > 0.71$ Å (below this point the diffraction pattern was dominated by background noise); the reflections 111, 110, 100 which lay outside the measured range were included at their calculated values, as was 000.

Table 1. Structural parameters from Rietveld refinement of cubic $NaMgF_3$ at 1223 K.

Space group	$Pm3m$				
a	3.949 95(1) Å[a]				
Na		Mg		F	
x	0[b]	x	1/2[b]	x	1/2[b]
y	0[b]	y	1/2[b]	y	1/2[b]
z	0[b]	z	1/2[b]	z	0[b]
U_{11}	0.0951(3) Å^2	U_{11}	0.0279(2) Å^2	U_{11}	0.1283(2) Å^2
				U_{33}	0.0266(3) Å^2
EXTN[c]	11.38(9) μm				
R_p	3.6%	R_{wp}	2.5%		
R_E	2.3%	χ^2	1.2		

[a] Cell parameter fixed during Rietveld refinement, e.s.d. given here is from earlier CAILS refinement (see text).
[b] Not varied.
[c] EXTN = extinction length (μm).
Figures in parentheses are estimated standard deviations, applying to the least significant figures.
$R_p = 100[\sum_i |Y_i(\text{obs.}) - Y_i(\text{calc})| / \sum_i Y_i(\text{obs.})]$
$R_{wp} = 100[\sum_i w_i |Y_i(\text{obs.}) - Y_i(\text{calc.})|^2 / \sum_i w_i Y_i^2(\text{obs.})]^{1/2}$
$R_E = 100[(N - P + C) / \sum_i w_i Y_i^2(\text{obs.})]^{1/2}$
$\chi^2 = \sum_i w_i |Y_i(\text{obs.}) - Y_i(\text{calc.})|^2 / (N - P + C)$

Classical molecular dynamics simulation (MDS) is now a well established technique for modelling the behaviour of solids [24–26]. It involves solving Newton's equations of motion for a set of atoms held in a 'simulation box', with the forces between atoms i and j calculated assuming a pair-wise interatomic potential of the form:

$$E_{ij}(\boldsymbol{r}_{ij}) = \frac{\boldsymbol{q}_i \cdot \boldsymbol{q}_j}{\boldsymbol{r}_{ij}} + A\mathrm{e}^{-\frac{r}{\rho}} - \frac{C}{r^6}$$

where the first term arises from Coulombic interactions from the charges (q) of the atoms, the second term models short-range repulsion and the final term is the van der Waals attractive force; A, ρ and C are constants. In this study, we utilized a constant stress 'molecular dynamics computer simulation of phase changes' (MDCSPC) code [27], running on the University of London Computing Consortium (ULCC) CONVEX, with periodic boundary conditions, using a time step of 10^{-15} s. All simulations were performed with a box containing 540 atoms ($3 \times 3 \times 3$ $Pbnm$ cells) with starting coordinates provided by a restart file written from a 387 K run which had been allowed to equilibrate for 5000 time steps. All subsequent simulations used 10 000 time-step runs, with the first 750 time steps discarded to allow equilibration. The potential parameters (table 2) were developed using the General Utility Lattice Program (GULP) [28]. Their basis was an interatomic potential for the binary system NaF which had previously been shown to produce good results [29], which was then

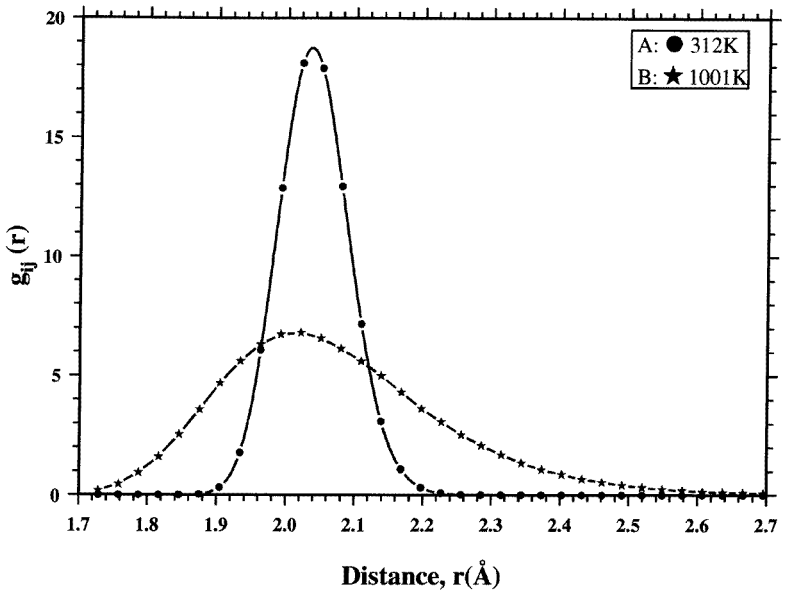

Figure 1. Mg–F pair radial distribution functions for $NaMgF_3$, estimated from molecular dynamics simulation (MDS) at: (A) 312 K; (B) 1001 K. The curves were calculated at the points shown, the lines being guides to the eye.

modified using experimental data for MgF_2 and $NaMgF_3$ [9, 30, 31] to which GULP fitted the potential parameters.

Table 2. Interatomic pair-potential parameters for $NaMgF_3$. For details see text.

	A (eV)	ρ (Å)	C (eV Å^6)
Na–F	1459.76	0.260	0.0
Mg–F	1617.52	0.258	0.0
F–F	1127.70	0.275	15.8

For the purposes of the present study, the most suitable method for ascertaining the behaviour of the Mg–F bond from the MDS was through the examination of the pair radial distribution function (RDF), defined as

$$g_{ij}(\boldsymbol{r}) = \frac{n_{ij}(\boldsymbol{r})}{4\pi r^2 (n_i n_j)^{0.5}}$$

where $n_{ij}(\boldsymbol{r})$ is the ensemble average of the number of ions of type j found within a shell of radius r with ion i at the centre and n_i and n_j are the bulk densities of ions of type i and j respectively. The first peak in the RDF between Mg and F in neighborite arises from the six Mg–F bonds in the MgF_6 octahedron; examination of the behaviour of this peak at different temperatures, therefore, shows how the distribution of Mg–F distances evolves.

As is commonly found in molecular dynamics simulation [32] T_m was estimated from our MDS at 1900 K, in poor agreement with experiment (1303 K). In order to allow comparison with the Fourier maps from the neutron diffraction study, an MDS was made at a temperature of 1841 K ($\approx 0.97 T_m$, as determined by MDS), with the atomic coordinates

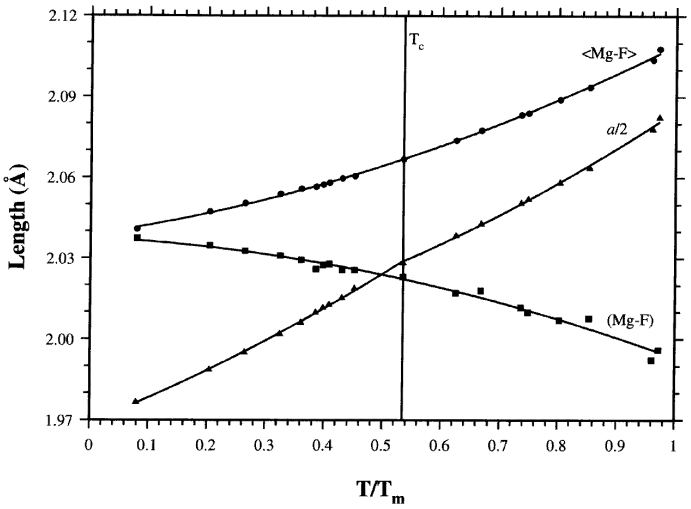

(a)

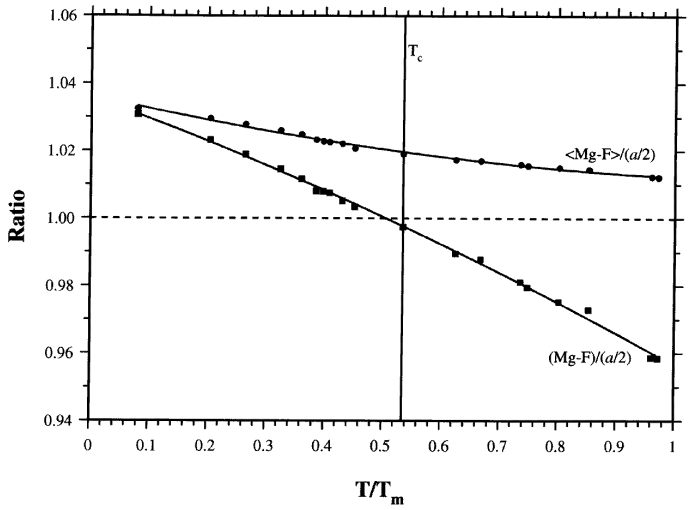

(b)

Figure 2. (a) Mean, ⟨Mg–F⟩, and mode (Mg–F) bond distances, pseudo-cubic and cubic cell parameters, estimated from MDS as a function of reduced temperature (T/T_m). In the orthorhombic phase ($T < T_c$) the pseudo-cubic cell parameter was estimated from $(V_o/4)^{1/3}$, where V_o is the volume of the orthorhombic cell. Note that on this reduced temperature scale T_c occurs at only 0.54, due to the overestimation of T_m. The lines shown as guides to the eye are second-order polynomials fitted to the data; for the cell parameter data separate curves were fitted above and below T_c. (b) Ratio of the mean, ⟨Mg–F⟩, and mode (Mg–F) bond distances to $a/2$, where a is the pseudo-cubic ($T < T_c$) or cubic ($T > T_c$) cell parameter. Note that (Mg–F)/($a/2$) approaches unity at $T = T_c$. The lines shown as guides to the eye are second-order polynomials fitted to the data.

output every 20 time steps after equilibration. This produced a file containing the coordinates of 250 020 atoms which were then reduced by lattice translations to a single cubic unit cell. The number density maps (figure 3) were then constructed by dividing this cell into cubes, 0.025 of the unit cell in size, and then counting the number of atoms within each cube.

Examination of the MDS results showed that, although the estimated value of T_m agreed poorly with experiment, the cell parameters indicated an orthorhombic $\rightarrow$ cubic transition with $T_c \approx 1020$ K, in very good agreement with the experimental value ($\approx$1040 K). Figure 1 shows the first peak in the Mg–F RDF from the MDS at two different temperatures, 312 K and 1001 K, the latter being at a point just below the $Pbnm \rightarrow Pm3m$ phase transition. It can be seen that although both RDFs are unimodal, that at 1001 K is much less symmetrical. At 1001 K the maximum in the curve (i.e. the mode of the distribution), which we shall denote by (Mg–F), is shifted to shorter bond distances, indicating a reduction in the most probable Mg–F bond length by an amount ($\approx$0.024 Å) similar to the apparent contraction in the Mg–F bond distance reported by Zhao *et al* [9]. However, at 1001 K the asymmetric distribution of nearest-neighbour Mg–F distances has a tail extending to larger values and the mean bond length, $\langle$Mg–F$\rangle$ ($=\int r 4\pi r^2 g(r)\,\mathrm{d}r$), is longer than at 312 K. Figure 2(a) shows the change in (Mg–F), $\langle$Mg–F$\rangle$ and in the pseudo-cubic and cubic cell parameter, a, estimated from the MDS, from 150 K to just below T_m. Figure 2(b) shows these two Mg–F distances as ratios of the cell parameter. As expected, at low temperatures (Mg–F) and $\langle$Mg–F$\rangle$ tend to become equal. As the temperature increases (Mg–F) decreases whereas $\langle$Mg–F$\rangle$ increases smoothly, with no sign of any reduction in length in the vicinity of the phase transition.

The physical origin of these changes in the distribution of bond distances can be seen most simply by examination of figure 3, which shows the number-density (MDS) and Fourier maps (neutron diffraction) of the average cubic structure, together with the results of the Rietveld refinement (table 1). The F^- ions are distributed extremely anisotropically in a flat disc elongated at right angles to the average Mg–F bond axis (i.e. perpendicular to one of the axes of the cubic unit cell). Qualitatively, the agreement between the MDS and diffraction study (figure 3) seems very good (it should be remembered that the two types of map are not exactly equivalent as the peaks in the Fourier maps are weighted according to the scattering lengths of the Na, Mg and F ions). Figure 4 shows the two principal cross sections of the distribution of F^- ions from MDS and from neutron diffraction, scaled to have the same maximum value; it can be seen that the results from the two methods are in excellent agreement, indicating that the MDS has produced a reliable representation of the average structure. The aspect ratio of the F^- ion distribution, as determined by the widths at half maximum, is 1.7. In both the MDS and neutron diffraction study, the maximum density of F^- ions occurs at the mid-point of the Mg–Mg line, i.e. their distribution resembles a discus, rather than a torus. If the displacements of the Mg and F ions were uncorrelated, this distribution would imply that the cell parameter, a, of the cubic structure above T_c should be given by 2(Mg–F). It is clear from figure 2(b) that this is not the case although, interestingly, the two quantities are almost exactly equal at $T = T_c$. It should, perhaps, also be mentioned at this point that there is formally no way in which a value of $\langle$Mg–F$\rangle$ may be extracted from diffraction data alone if only the Bragg reflections are measured; these contain information about the spatially and temporally averaged structure and give no information about the correlations between the displacements of neighbouring atoms. In a framework structure, such as a perovskite, the atomic displacements arising from rotational modes of the octahedra *must* be correlated. If the behaviour of the material is to be properly understood, it is, therefore, necessary to combine diffraction studies with techniques such as MDS (or possibly to measure and model the total diffraction pattern, including the diffuse

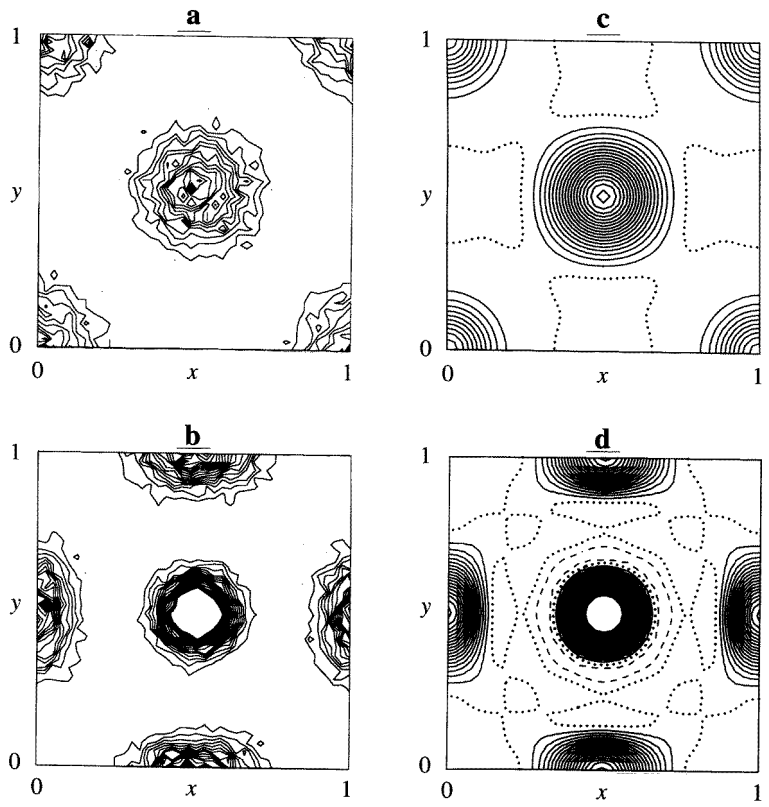

Figure 3. Cross sections of the $NaMgF_3$ cubic unit cell, at $z = 0$ and $z = 0.5$, with atomic coordinates as defined in table 1. (a, b) Number-density maps from MDS, $T = 0.97T_m$. (c, d) Neutron scattering length density maps, $T = 0.94T_m$. The disc-like density of the F^- ions is viewed face-on in (a) and (c) (F^- at 1/2, 1/2, 0) and edge-on in (b) and (d) (F^- at 1/2, 0, 1/2 and 0, 1/2, 1/2). Contour levels in (a) and (b) are every 5 atoms and in (c) and (d) every 0.05×10^{-12} cm $Å^{-3}$. In both (b) and (d), the density at the centre of the Mg ion lies above the maximum contour level shown.

scattering); the corrections for isotropic, uncorrelated thermal motion applied to the bond distances in previous work [9] have little validity for a structure of this type.

Our results strongly suggest that the major component of the anisotropic distribution of the F^- ions arises from optic rotational modes of the coupled MgF_6 octahedra, with adjacent octahedra rotating in opposite directions so as to bend the Mg–F–Mg bonds. These motions have the effect, for a fixed Mg–F bond length, of reducing the distance between the Mg ions in neighbouring octahedra, thus leading to a pseudo-cubic or cubic cell parameter of less than $2\langle$Mg–F$\rangle$. In the orthorhombic phase these rotations have both a static component (the octahedral tilts) and a dynamic component from thermal motion; in the cubic phase only the dynamic component remains. In view of the fact that $NaMgF_3$ undergoes a phase transition in which octahedral tilts 'freeze in', this conclusion is in no way surprising. What is of interest, however, is the size of the dynamic contribution to the change in cell parameter and the range of temperature over which it persists.

The anomalous bond lengths reported by Zhao *et al* [9, 12] seem, therefore, clearly

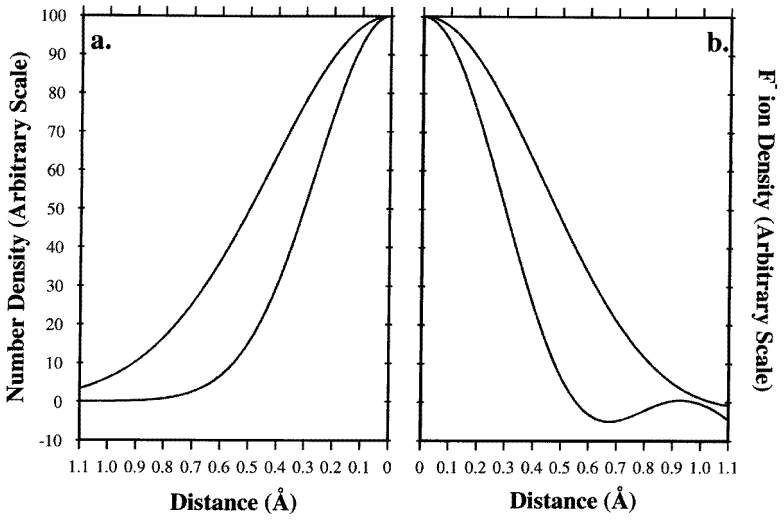

Figure 4. Principal cross sections of the F^- ion density (arbitrary scale): (a) from MDS; (b) from neutron diffraction. The curves shown in (a) were obtained by fitting Gaussian functions to the data shown in figure 3(c); those in (b) are a smooth curve drawn through the values of the Fourier map.

to arise from very large dynamic displacements of the F^- ions, almost certainly associated with soft optic modes responsible for the $Pbnm \rightarrow Pm3m$ phase transition. The volumetric effect of this 'dynamic lattice contraction' in the cubic phase of $NaMgF_3$ just above T_c was estimated from our MDS to be 0.48 Å^3, or 6%, whilst just below T_m it was 0.33 Å^3 (4%), with the average angle of tilt of the octahedra ($=\cos^{-1}[(a/2)/\langle \mathrm{Mg–F} \rangle]$) equal to 11° and 9° respectively. The cubic phase of perovskites such as $NaMgF_3$ at high temperatures is, therefore, probably best visualized in terms of a time-averaged structure in which, instantaneously on a unit-cell scale, the octahedra are tilted and/or distorted to give local structures of lower symmetry. The extent to which this affects the cell parameter will vary for different materials; for example, our preliminary investigations of $KMgF_3$ (unpublished), which is cubic at all temperatures, indicate that the distribution of F^- ions is much less anisotropic than in $NaMgF_3$, suggesting, as might be expected, that the effect is larger in perovskites with soft-mode condensation. It should be noted that cubic and orthorhombic perovskite structures might be expected to respond quite differently to the dynamic component of the octahedral tilting. In the cubic phase there is no static tilt and thus any thermally induced bending of the Mg–F–Mg bond will reduce the size of the cell parameter. In the orthorhombic phase, however, in which the static tilts are non-zero, the dynamic tilts will, to first order, have no effect on the size of the cell, since the thermal motion will both increase and decrease the Mg–F–Mg bond angle. These considerations may well, therefore, be of importance for *a priori* simulations of perovskites which do not include explicitly the thermal motions of the atoms. In particular, simulations of $MgSiO_3$ performed at 0 K [4, 5] may well overestimate the stability of the orthorhombic phase with respect to the cubic phase.

We should like to thank Dr J A Stuart for assistance with the preparation of the sample of $NaMgF_3$, Dr Robin Grimes and Dr S Vyas for assistance with the development of

the interatomic potential and Dr J Brodholt for assistance with the molecular dynamics simulations.

References

[1] Ringwood A E 1962 *J. Geophys. Res.* **67** 4005–10
[2] Hemley R J and Cohen R E 1992 *Annu. Rev. Earth Planet. Sci.* **20** 553–600
[3] Vocadlo L, Patel A and Price G D 1995 *Miner. Mag.* **59** 597–605
[4] Wentzcovitch R M, Martins J L and Price G D 1993 *Phys. Rev. Lett.* **70** 3947–50
[5] Wentzcovitch R M, Ross N L and Price G D 1995 *Phys. Earth Planet. Int.* **90** 101–12
[6] Poirier J P, Peyronneau J, Gesland J Y and Brébec G 1983 *Phys. Earth Planet. Int.* **32** 273–87
[7] Chao E C T, Evans H T, Skinner B J and Milton C *Am. Mineral.* **46** 379–93
[8] Zhou L X, Hardy J R and Cao H Z 1997 *Geophys. Res. Lett.* **24** 747–50
[9] Zhao Y, Weidner D J, Parise J B and Cox D E 1993 *Phys. Earth Planet. Int.* **76** 1–16
[10] Zhao Y, Weidner D J, Parise J B and Cox D E 1993 *Phys. Earth Planet. Int.* **76** 17–34
[11] Zhao Y, Parise J B, Wang Y, Kusaba K, Vaughan M T, Weidner D J, Kikegawa T, Chen J and Shimomura O 1994 *Am. Mineral.* **79** 615–21
[12] Zhao Y, Weidner D J, Ko J, Leinenweber K, Liu X, Li B, Meng Y, Pacalo E G, Vaughan M T, Wang Y and Yeganeh-Haeri A 1994 *J. Geophys. Res.* **99** 2871–85
[13] O'Keeffe M and Bovin J-O 1979 *Science* **206** 599–600
[14] Andersen N H, Kjems J K and Hayes W 1985 *Solid State Ion.* **17** 143–5
[15] Cheesman P A and Angell C A 1981 *Solid State Ion.* **5** 597–600
[16] Matsui M and Price G D 1991 *Nature* **351** 735–7
[17] Lines M E and Glass A M 1977 *Principles and Applications of Ferroelectrics and Related Materials* (Oxford: Clarendon)
[18] Darlington C N W 1996 *Phys. Status Solidi* a **155** 31–42
[19] Glazer A M 1972 *Acta Crystallogr.* B **28** 3385–92
[20] Aleksandrov K S 1976 *Ferroelectrics* **14** 801–5
[21] Brown P J and Matthewman J M 1987 *Rutherford Appleton Laboratory Report* RAL-87-010
[22] Brown P J and Matthewman J M 1990 *Rutherford Appleton Laboratory Report* RAL-90-021
[23] Brown P J and Matthewman J M 1993 *Rutherford Appleton Laboratory Report* RAL-93-009
[24] Dove M 1988 *Physical Properties and Thermodynamic Behaviour of Minerals (NATO ASI Series C 225)* ed E K H Salje (Dordrecht: Riedel)
[25] Matsui M 1988 *Phys. Chem. Miner.* **16** 234–8
[26] Wall A, Price G D and Parker S C 1986 *Miner. Mag.* **50** 693–707
[27] Smith W 1991 *Daresbury Laboratory Technical Memorandum* DL/SCI/TM84T
[28] Gale J D 1997 *J. Chem. Soc. Faraday Trans.* **93** 629–37
[29] Dornford-Smith A and Grimes R W 1995 *Phil. Mag.* **72** 563–76
[30] Kandil H M, Greiner J D, Ayers A C and Smith J F 1981 *J. Appl. Phys.* **52** 759–63
[31] Zhao Y H and Weidner D J 1993 *Phys. Chem. Miner.* **20** 419–24
[32] Vocadlo L and Price G D 1996 *Phys. Chem. Miner.* **23** 42–9